ISSN 2070-2051, Protection of Metals and Physical Chemistry of Surfaces, 2011, Vol. 47, No. 5, pp. 590–597. © Pleiades Publishing, Ltd., 2011.
Original Russian Text © A.V. Syugaev, S.F. Lomaeva, N.V. Lyalina, S.M. Reshetnikov, 2011, published in Fizikokhimiya Poverkhnosti i Zashchita Materialov, 2011, Vol. 47, No. 5, pp. 486–483.

NANOSCALE AND NANOSTRUCTURED MATERIALS AND COATINGS

Corrosion–Electrochemical Properties of α-Fe + Fe_3C + TiC Nanocomposites in Neutral Environments

A. V. Syugaev[a], S. F. Lomaeva[a], N. V. Lyalina[a], and S. M. Reshetnikov[b]

[a] *Physical-Technical Institute, Ural Division, Russian Academy of Sciences, ul. Kirova 132, Izhevsk, 426000, Russia*
e-mail: uds@pti.udm.ru

[b] *Udmurt State University, ul. Universitetskaya 1, Izhevsk, 426034 Udmurtia, Russia*
e-mail: smr41@mail.ru

Received May 28, 2010

Abstract—The corrosion–electrochemical properties of α-Fe + Fe_3C + TiC three-phase nanocrystalline composites in borate solutions with pH 6.3–9.0 both with and without NaCl are studied. α-Fe + Fe_3C + TiC composites are found to have heightened resistances at active-oxidation potentials of α-Fe and cementite due to the formation of $xFeO \cdot yTiO_2$ mixed surface oxides. The protective properties of passive films based on $xFeO \cdot yTiO_2$ and their resistance to local activation are worse than those of Fe_3O_4/γ-Fe_2O_3 (γ-FeOOH) passive films formed on iron and α-Fe + Fe_3C composites.

DOI: 10.1134/S2070205111050182

INTRODUCTION

It was shown that the resistance of α-Fe + Fe_3C + TiC three-phase composites against acids is not high because of the high activity of carbide inclusions with respect to hydrogen reduction and the low protective ability of the passive films 2]. Free carbon, which is accumulated on the surface during the active dissolution of α-Fe + Fe_3C + TiC composites in the active potential range, has a negative effect on the structure and protective properties of passive films.

The object of this work was to study the effect of the structure state on the electrochemical properties of nanocrystalline α-Fe + Fe_3C + TiC composites in borate solutions with and without chloride ions in a pH range of 6.3–9.0, as well as to clarify the role of titanium carbide in the passivation and local activation of the composites.

EXPERIMENTAL

Composites were produced by the mechanochemical synthesis in a Fritsch P-7 planetary ball mill, and the powders were compacted by magnetic pulse pressing [3–5]. The following conditions were used:

(i) 70 : 15 : 15 at. % mixture of iron, titanium, and graphite powders; argon environment; duration of mechanochemical synthesis t_{MS} = 16 h (Fe70Ti15C15 specimen);

(ii) 70 : 30 at. % mixture of iron and TiC carbide powders; argon environment; t_{MS} = 16 h (Fe(70)TiC(30) specimen);

(iii) 70 : 15 at. % mixture of iron and titanium powders; toluene environment; t_{MS} = 20 and 32 h (Fe70Ti15/tol20 and Fe70Ti15/tol32 specimens); and

(iv) 70 : 15 at. % mixture of iron and titanium powders; toluene environment containing 3% vinyltriethoxysilane (VTES); t_{MS} = 32 h (Fe70Ti15/VTES specimen).

According to the data of [2–5], composites are in a nanocrystalline state with an α-Fe grain size of 10–15 nm. The iron lattice parameter of most specimens falls in the range a = 0.2872–0.2874 nm, which is larger than the individual iron lattice constant due to the presence of up to 2 at. % titanium in the form of a solid solution in iron. Carbide inclusions have sizes of 20–100 nm and are homogeneously distributed over the surfaces of α-Fe+Fe_3C + TiC composites. The number of carbide phases is given in Table 1.

When interpreting the obtained electrochemical data, we used reference specimens of Armco iron (8×10^{-3} C, 5×10^{-3} S, 3×10^{-3} P, 3×10^{-2} O, and 6×10^{-3} wt % Mn) and cementite, which was obtained according to the method outlined in [6].

X-ray photoelectron spectra were recorded with an ES-2401 spectrometer with an Mg anode. The E_b bond energy of the C1s electrons in the alkyl group was assumed to be 285.0 eV. The ionic etching of the sur-

Table 1. Phase composition of composites (wt %, ±5%)

Specimen	α-Fe	TiC	Fe_3C
Fe(70)TiC(30)	67	19	14
Fe70Ti15C15	44	20	36
Fe70Ti15/tol20	52	21	27
Fe70Ti15/tol32	30	19	51
Fe70Ti15/VTES	22	14	64

face was carried out using an Ar^+ ion beam with an energy of 1 kV at a current of 15 μA. Under these etching conditions, a surface layer with a thickness of 10 Å is removed in 1 min. The deconvolution of the spectra was carried out according to the method of [7].

Polarization measurements were carried out under potentiodynamic conditions on an IPC-Pro potentiostat in a conventional electrochemical cell CEC-2 at room temperature with natural aeration. A silver-chloride electrode was taken as the reference electrode and a platinum electrode was taken as the auxiliary electrode. All potentials are given with respect to the standard hydrogen electrode and currents are recalculated to the visible surface of specimens. Specimens were insulated in Epoxy resin. The treatment of the surface before measurements consisted of sandpapering and additional polishing with Al_2O_3 powder wetted with distilled water. Borate solutions (0.3 M H_3BO_3 + 5 M NaOH) with pH 6.3, 7.4, 8.3, and 9.0 were taken as model environments. Pit-formation processes were studied in a borate solution with pH 7.4 containing NaCl additives (10^{-4} to 0.5 M). Solutions were prepared from chemically pure reagents and distilled water.

Specimens were exposed to model solutions for 1 h; then, they were cathodically polarized at −800 mV for 10 min, during which potentiodynamic curves were recorded at a rate of 1 mV/s. When local activation was studied, the specimens were polarized from the corrosion potential at a rate of 0.5 mV/s.

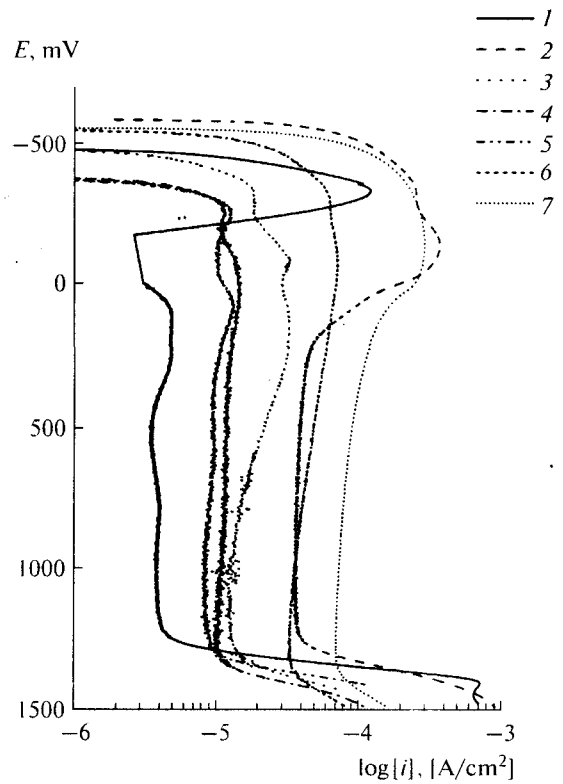

Fig. 1. Anodic curves on (*1*) Armco Fe, (*2*) cementite, and (*3*–*7*) α-Fe + Fe_3C + TiC composites: (*3*) Fe70Ti15C15, (*4*) Fe(70)TiC(30), (*5*) Fe70Ti15/tol20, (*6*) Fe70Ti15/tol32, and (*7*) Fe70Ti15/VTES in borate solution with pH 7.4.

RESULTS AND DISCUSSION

Peculiarities of Oxidation and Passivation of α-Fe + Fe_3C + TiC Composites

Figure 1 shows anodic curves of α-Fe + Fe_3C + TiC composites, Armco Fe, and Fe_3C in a borate solution with pH 7.4. The intense dissolution of ferrite phase proceeds at a potential of −300 mV, while that of Fe_3C, at $E \sim -100$ mV. At all studied pH values in the range of 6.3–9.0, the oxidation currents of α-Fe + Fe_3C + TiC composites increase with an increase in the cementite content, which is related to the increased defectiveness of the oxide films formed on Fe_3C inclusions [6, 8].

Let us compare anodic curves of α-Fe + Fe_3C + TiC three-phase and α-Fe + Fe_3C two-phase composites that contain nearly the same amount of cementite (Fig. 2, Table 2). On α-Fe + 27% Fe_3C composite, pronounced peaks that correspond to the successive oxidation of ferrite and cementite are seen, while on the three-phase composite with the same cementite content, these peaks are absent and the dissolution currents are smaller by a factor of five. At the same time, in the passivation range, the oxidation rate of the

Table 2. Current densities (μA/cm², ±5%) at passivation onset potentials (i_{po}) on α-Fe and Fe_3C and at complete passivation (i_{cp}) on α-Fe + Fe_3C + TiC and α-Fe + Fe_3C composites in borate solutions at various pH

Specimen composition	i_{po}(α-Fe)		$i_{po}(Fe_3C)$		i_{cp}	
	pH 6.3	pH 7.4	pH 6.3	pH 7.4	pH 6.3	pH 7.4
α-Fe + 14%Fe_3C + 19%TiC	44	8	30	13	24	11
(α-Fe + 12%Fe_3C)	(200)	(100)	(100)	(30)	(5)	(4)
α-Fe + 27%Fe_3C + 21%TiC	73	8	30	10	23	9
(α-Fe + 27%Fe_3C)	(175)	(50)	(190)	(37)	(9)	(4)
α-Fe + 51%Fe_3C + 19%TiC	81	62	122	71	68	36
(α-Fe + 55%Fe_3C)	(130)	(270)	(53)	(57)	(18)	(9)

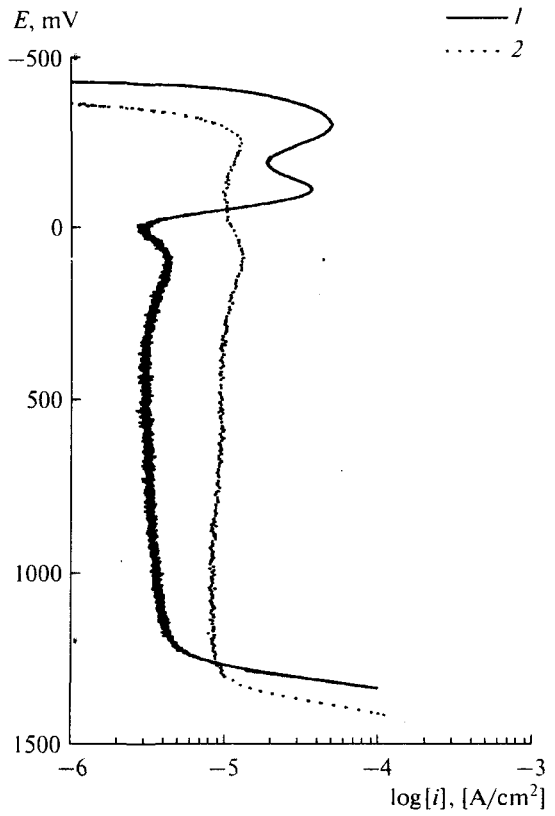

Fig. 2. Anodic curves on composites with close cementite contents: (1) α-Fe + 27% Fe_3C and (2) α-Fe + 27% Fe_3C + 21% TiC in borate solution with pH 7.4.

three-phase composite is higher. These peculiarities indicate that the structure of oxide layers formed during the oxidation of composites is different. Note that, with an increase in the cementite content, the difference between the anodic behavior of the three- and two-phase systems decreases (Table 2).

In order to clarify the nature of the passive film on α-Fe + Fe_3C + TiC, XPE spectra of Fe70Ti15/tol20 and Fe70Ti15/VTES specimens were recorded that are characterized by the minimal and maximal anodic currents. Armco Fe was considered for comparison. Passive films were obtained by anodic polarization at a potential of 500 mV in a borate solution with pH 7.4. The spectra are shown in Fig. 3, and the data of a quantitative analysis of the surface layers are given in Table 3.

In C1s spectra, the line at E_b ~ 283.0 eV corresponds to Fe_3C [9], the line at E_b ~ 285.0 eV corresponds to the alkyl-group carbon, and the line at E_b > 286.0 eV corresponds to the carbon of oxygen-containing organic groups [10]. O1s spectra of all specimens, regardless of ionic etching, are similar and involve lines that correspond to oxides (E_b ~ 530.0 eV) and hydroxides (E_b ~ 531.5 eV) [10].

In Fe2p spectra, the signal at E_b ~ 707.0 eV corresponds to α-Fe and Fe_3C, E_b ~ 709.5 eV corresponds to FeO, E_b ~ 708.3 and 710.6 eV corresponds to Fe_3O_4, E_b ~ 711.0 eV corresponds to Fe_2O_3, and E_b ~ 712.0 eV corresponds to FeOOH. In Fe3p spectra, the line at E_b ~ 53.0 eV corresponds to α-Fe and Fe_3C, E_b ~ 54.9 eV corresponds to FeO, E_b ~ 53.9 and 55.9 corresponds to Fe_3O_4, E_b ~ 55.7 eV corresponds to Fe_2O_3, and E_b ~ 56.6 eV corresponds to FeOOH [9–11]. Fe3p electrons are characterized by a greater escape depth, which makes it possible to study the composition of the deeper layers [12].

In Ti2p spectra, the line at E_b ~ 454.0 eV corresponds to Ti, E_b ~ 454.8 eV corresponds to TiC, E_b ~ 458.2 eV corresponds to mixed MeO TiO_2 oxides, and E_b ~ 459.0 eV corresponds to TiO_2 [10]. In the B1s spectrum, the signal at E_b ~ 191.8 eV corresponds to boric-acid derivatives [10].

In Fe3p and Fe2p spectra of Armco Fe (Fig. 3, curve *1*), the presence of a signal of nonoxidized iron means that the thickness of the oxide film is no larger than that of the analyzed layer, i.e., no more than 3–5 nm [12]. The main components of Fe2p and Fe3p spectra can be assigned to Fe_3O_4 and Fe_2O_3, which well agrees with the conventional concept of the formation of an Fe_3O_4/γ–Fe_2O_3 two-phase passive film on iron [13]. C1s spectrum of Armco iron is typical of hydrocarbon compounds adsorbed on the surface.

In Fe2p and Fe3p spectra of the passive film formed on Fe70Ti15/tol20 (Fig. 3, curve *2*), there is no signal that corresponds to α-Fe or Fe_3C, which means that the passive film is thicker than that on Armco Fe. In

Table 3. Compositions of surface layers of passive films formed on Armco Fe and Fe70Ti15/tol20 and Fe70Ti15/VTES composites

Specimen	Etching duration, min	Element content, at. %						
		B	C	O	Fe	Ti	Si	Fe/Ti
Armco Fe	1	0	25	49	26			
Fe70Ti15/tol20	1	9	19	49	19	4		4.8
	20	0	28	28	36	8		4.5
Fe70Ti15/VTES	1	0	39	44	17	traces	0	
	20	0	29	44	27	traces	0	

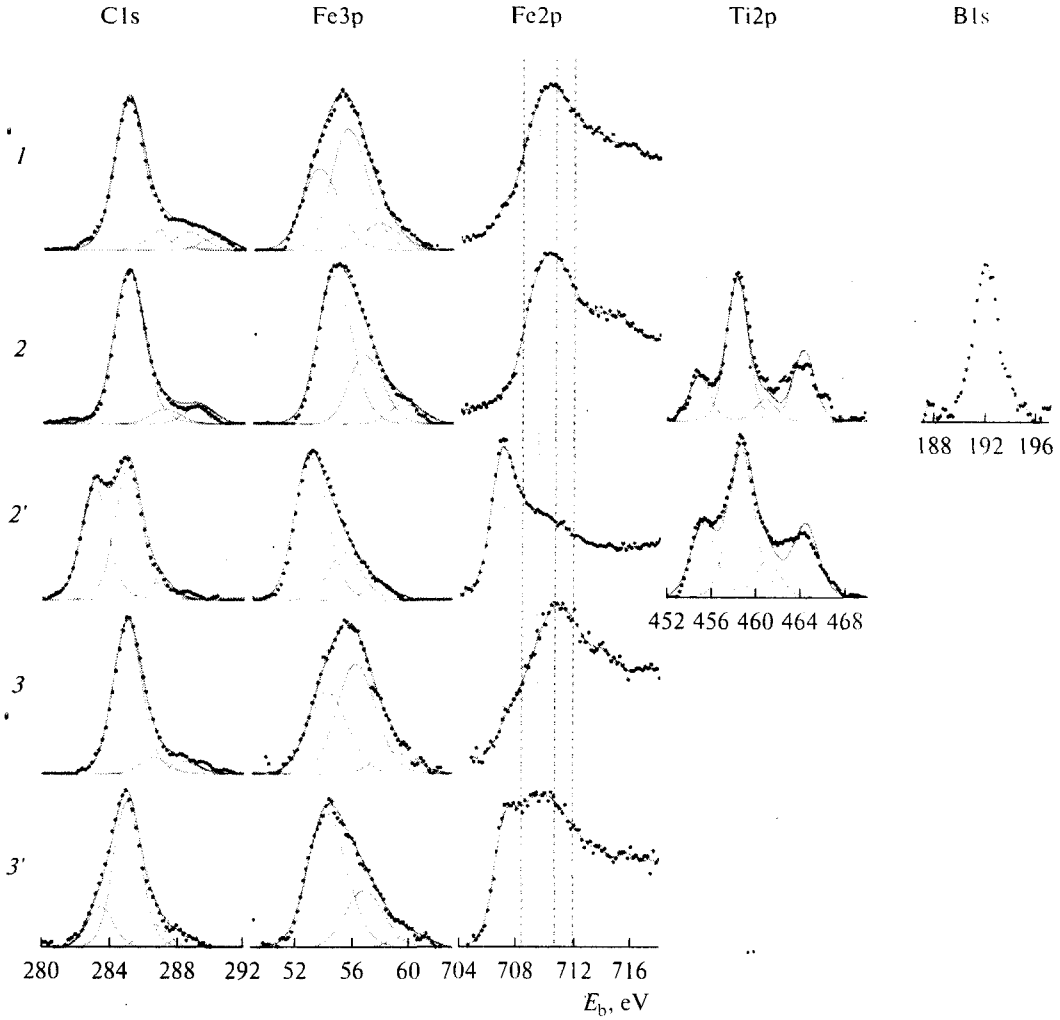

Fig. 3. XPE spectra of passive films formed on (*1*) Armco Fe, (*2*, *2'*) Fe70Ti15/tol20, and (*3*, *3'*) Fe70Ti15/VTES composites, upon ionic etching, min: (*1*–*3*) 1 and (*2'*, *3'*) 20.

the Fe3p spectrum, the line at E_b = 54.6 eV corresponding to Fe(II) has the highest intensity. However, the position of the line is atypical of the reference Fe_3O_4 and FeO oxides. Insofar as the main contribution to the Ti2p spectrum comes from the line at E_b = 458.2 eV, which is typical of MeO · TiO_2 mixed oxides, we can conclude that Fe(II) is involved in xFeO · $y$$TiO_2$ oxides. The presence of a single peak in the B1s spectrum indicates the adsorption of boric acid derivatives on the passive film; the signal disappears upon ionic etching. Furthermore, upon etching (Fig. 3, *2*, Table 3), the amount of oxygen decreases, while the content of carbon, iron, and titanium increases. Upon ionic etching, the signals of α-Fe and Fe_3C prevail in Fe3p and Fe2p spectra; an intense line at E_b = 283.0 eV corresponding to Fe_3C appears in C1s spectrum; and the intensity of a line corresponding to TiC increases in the Ti2p spectrum, which means that the passive film was almost completely removed. The Fe/Ti ratio before and after etching corresponds to the original composition of the specimen; i.e., the surface does not become enriched in either iron or titanium during the oxidation.

In a passive film formed on Fe70Ti15/VTES specimen, there is no silicon, while titanium is present in trace amounts, even upon ionic etching. A peculiarity of the Fe3p and Fe2p spectra is the increased content of hydroxides (Fig. 3, curve *3*). Upon ionic etching, the intensities of the lines at E_b = 707.7 eV in the Fe2p spectrum and E_b = 54.2 eV in the Fe3p spectrum increase (Fig. 3, curve *3*), and a signal at E_b = 283.4 eV appears in the C1s spectrum. These signals can be assigned to $Fe_3C_{1-x}O_x$ ($x < 1$) iron oxycarbides. Oxy-

carbides are seemingly intermediate products of the anodic oxidation of cementite as follows:

$$Fe_3C + xH_2O \rightarrow Fe_3C_{1-x}O_x + xC + 2xH^+ + 2xe, \quad x < 1; \tag{1}$$

$$Fe_3C_{1-x}O_x + (6-x)H_2O \rightarrow 3Fe(OH)_2 + (1-x)C + (6-2x)H^+ + (6-2x)e, \quad x < 1. \tag{2}$$

Quantitative analysis indicates the formation of $Fe_3C_{1-x}O_x$ with $x \sim 0.3$. A passive film on the Fe70Ti15/VTES composite is thicker than that on Fe70Ti15/tol20, which is indicated by the substantial contribution of oxides and hydroxides to Fe2p spectrum recorded after ionic etching.

Thus, the peculiarity of the passivation of α-Fe + Fe_3C + TiC composites is the formation of $xFeO \cdot yTiO_2$ mixed oxides in the surface layer, which decrease the currents in the active-oxidation range of ferrite and cementite. With an increase in the cementite content in the composites, the part of $xFeO \cdot yTiO_2$ oxides in the passive films decreases and the part of hydroxides increases, which decreases the protective properties of the passive films.

Mechanisms of Protective Effect of $xFeO \cdot yTiO_2$ Mixed Oxides

Let us consider the possible mechanisms of the formation of $xFeO \cdot yTiO_2$ oxides and their effect on the passivation of α-Fe + Fe_3C + TiC composites. First, $xFeO \cdot yTiO_2$ mixed oxides form during the primary oxidation of the ferrite phase doped with Ti atoms as follows:

$$FeTi_y + (2 + 2y - x)H_2O \rightarrow xFeOyTiO_2 + (1-x)Fe(OH)_2 + (2+4y)e. \tag{3}$$

Furthermore, they can form at the boundaries of TiC inclusions, which are covered with a TiO_2 layer, as follows [14]:

$$xFe + yTi_2 + xH_2O \rightarrow xFeOyTiO_2 + 2xH^+ + 2xe. \tag{4}$$

$xFeO \cdot yTiO_2$ mixed oxides, which are formed at the first stage of the oxidation of composites according to Eqs. (3) and (4), have protective properties. Therefore, there is no pronounced peak that corresponds to the oxidation of either ferrite or cementite in the curves.

Second, similar to iron and α-Fe + Fe_3C, the passivation of α-Fe + Fe_3C + TiC is determined by the formation of γ-Fe_2O_3. However, in the presence of $xFeO \cdot yTiO_2$, the reaction, which is responsible for the transition of the composite to the stable passive state, changes. On iron and two-phase composites, the complete passivation proceeds near the equilibrium potential of the following reaction [8, 13]:

$$2Fe_3O_4 + H_2O \rightarrow 3\gamma\text{-}Fe_2O_3 + 2H^+ + 2e; \tag{5}$$

$$E_{eq} = 580 - 59\ pH\ (mV), \tag{6}$$

whereas, on three-phase composites, TiO_2 and $xFeO \cdot yTiO_2$ mixed oxides can be involved in the reaction ($xFeO \cdot yTiO_2$ is normalized to one FeO mole) as follows:

$$2FeO\,y/x\,TiO_2 + H_2O \rightarrow \gamma\text{-}Fe_2O_3 + 2\,y/x\,TiO_2 + 2H^+ + 2e. \tag{7}$$

The thermodynamic estimation of the known x and y values [15] shows that the equilibrium potential of reaction (7) is more negative than that of reaction (5) by 200–300 mV. Then, in the presence of TiO_2 and $xFeO \cdot yTiO_2$, the range of the electrochemical stability of γ-Fe_2O_3 is broader, which facilitates the passivation of α-Fe + Fe_3C + TiC composite compared to iron and α-Fe + Fe_3C composite.

If the second supposition is valid, the heightened corrosion potentials ($\sim E_{corl}$) of the most stable Fe70Ti15/tol20 and Fe(70)TiC(30) composites, which are close to the equilibrium formation potential of γ-Fe_2O_3, can be explained as follows:

$$2Fe(OH)_2 \rightarrow \gamma - Fe_2O_3 + H_2O + 2H^+ + 2e; \tag{8}$$

$$E_{eq} = 62 - 59\ pH\ (mV). \tag{9}$$

According to Eq. (5), the complete passivation potential is substantially lowered and, as a result, the following relation is valid for α-Fe + Fe_3C + TiC composites: $\sim E_{cor} = \sim E_{po} = E_{cp}$; complete passivation is achieved at E_{corl} of the specimens. In this case, passive films with a smaller thicknesses than those on iron and α-Fe + Fe_3C composites should be formed because of the absence or small thickness of the magnetite sublayer.

Actually, the recorded X-ray photoelectron spectra indicate that passive films formed on composites are thicker than those on Armco iron. Furthermore, there is no noticeable contribution from γ-Fe_2O_3 and TiO_2 to the spectra, though the oxides should be present in the passive film according to Eq. (7). This means that the supposition about the change in the reaction responsible for the electrochemical stabilization of γ-Fe_2O_3 is less probable than the direct protective effect provided by $xFeO \cdot yTiO_2$ mixed oxides.

Local Activation of α-Fe + Fe_3C + TiC Composites

Polarization curves of α-Fe + Fe_3C + TiC composite, Armco Fe, and Fe_3C cementite recorded in a 10^{-2} M NaCl solution are shown in Fig. 4. In the presence of 10^{-2} M NaCl, a passive film is retained on Armco iron and cementite. At anodic polarization, both specimens undergo local activation, and the local-activation potential (E_{la}) of cementite is higher than that of Armco Fe by 300 mV.

According to the behavior in NaCl, α-Fe + Fe_3C + TiC composites can be divided into two groups depending on the cementite content. Specimens of the first group that contain less than 50% cementite

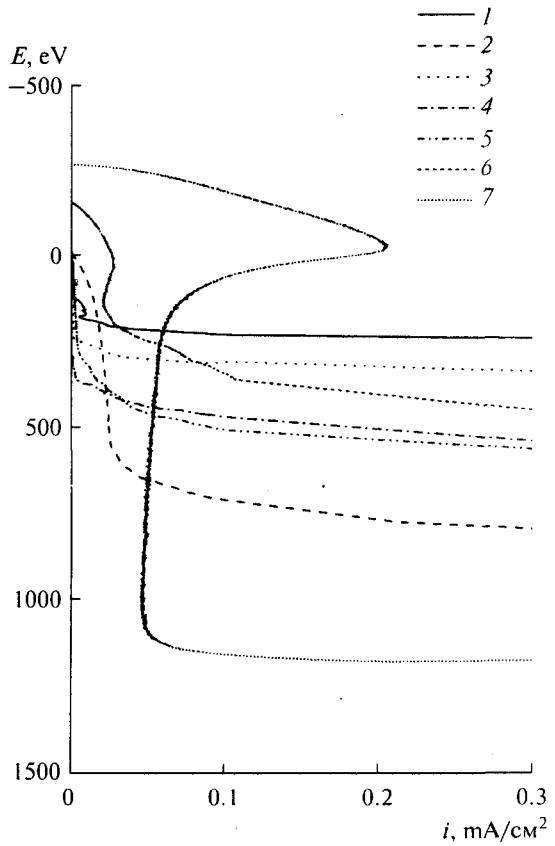

Fig. 4. Anodic curves on (*1*) Armco Fe, (*2*) cementite, and (*3–7*) α-Fe + Fe_3C + TiC composites: (*3*) Fe(70)TiC(30), (*4*) Fe70Ti15C15, (*5*) Fe70Ti15/tol20, (6) Fe70Ti15/tol32, and (*7*) Fe70Ti15/VTES in borate solution with pH 7.4 containing 10^{-2} M NaCl.

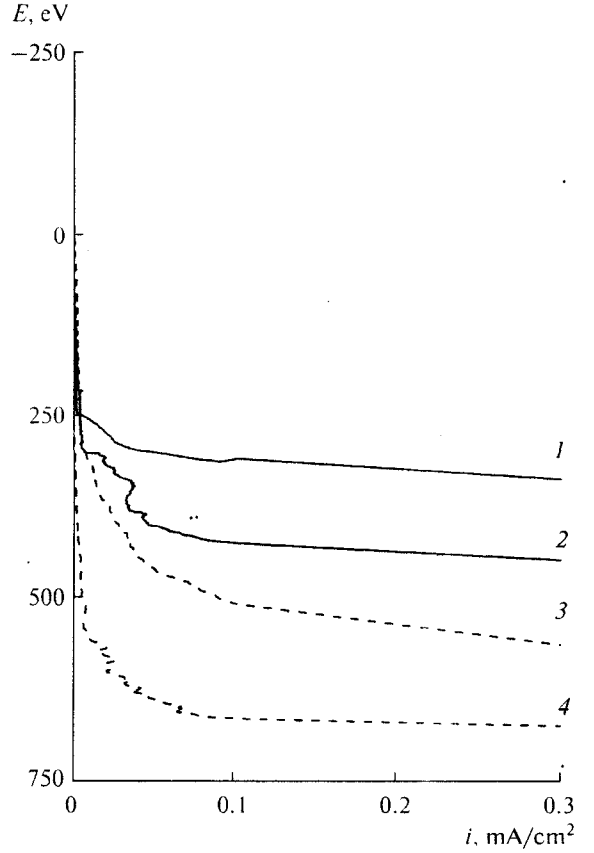

Fig. 5. Anodic curves on composites with close cementite contents: (*1*) α-Fe + 16% Fe_3C and (2) α-Fe + 14% Fe_3C + 19% TiC; (*3*) α-Fe + 27% Fe_3C, and (*4*) α-Fe + 27% Fe_3C + 21% TiC in borate solution with pH 7.4 containing 10^{-2} M NaCl.

are not depassivated in a 10^{-2} M NaCl solution. According to the E_{la} values, specimens can be ranked as follows: Armco Fe < Fe(70)TiC(30) < Fe70Ti15C15 ~ Fe70Ti15/tol20 < Fe_3C. The same series reflects the increase in the cementite content in the specimens.

The second group of specimens that contain more than 50% cementite are depassivated in 10^{-2} M NaCl. This results in the low E_{cor} values and the appearance of activation peaks at anodic polarization, which can be assigned to either the oxidation of the cementite component or the additional oxidation of the passive film to FeOOH. Further anodic polarization causes the local activation of only the Fe70Ti15/tol32 specimen. On the Fe70Ti15/VTES specimen, a high-intensity anodic peak is recorded that corresponds to the formation of a substantially thick oxide layer that prevents the local activation.

Let us compare the resistance of passive films, which are formed on two- and three-phase composites with close cementite contents, against local activation (Fig. 5) 16]. Passive films differ in their chemical nature. On three-phase composites, E_{la} values are 100–200 mV lower, which means that $xFeO \cdot yTiO_2$ passive films are more susceptible to chloride attack compared to $Fe_3O_4/\gamma\text{-}Fe_2O_3$ (γ-FeOOH) passive films on α-Fe + Fe_3C composites.

The effect of NaCl concentration on the anodic processes can be considered by an example of Fe70Ti15C15 specimen compared to Armco Fe and Fe_3C cementite (Fig. 6). At low chloride concentrations, Fe70Ti15C15 composite undergoes local activation at the same concentration as cementite, i.e., 10^{-2} M, while Armco Fe is activated at just 10^{-3} M NaCl.

At high NaCl concentrations, Armco Fe is depassivated at 0.5 M, while cementite is depassivated at 0.1 M. At the same time, Fe70Ti15C15 composite is not depassivated in the range of 0.1–0.5 M NaCl, which means that $xFeO \cdot yTiO_2$ is not completely removed from the surface, even in concentrated chloride solutions. However, the local activation of the Fe70Ti15C15 specimen takes place near the corrosion potential.

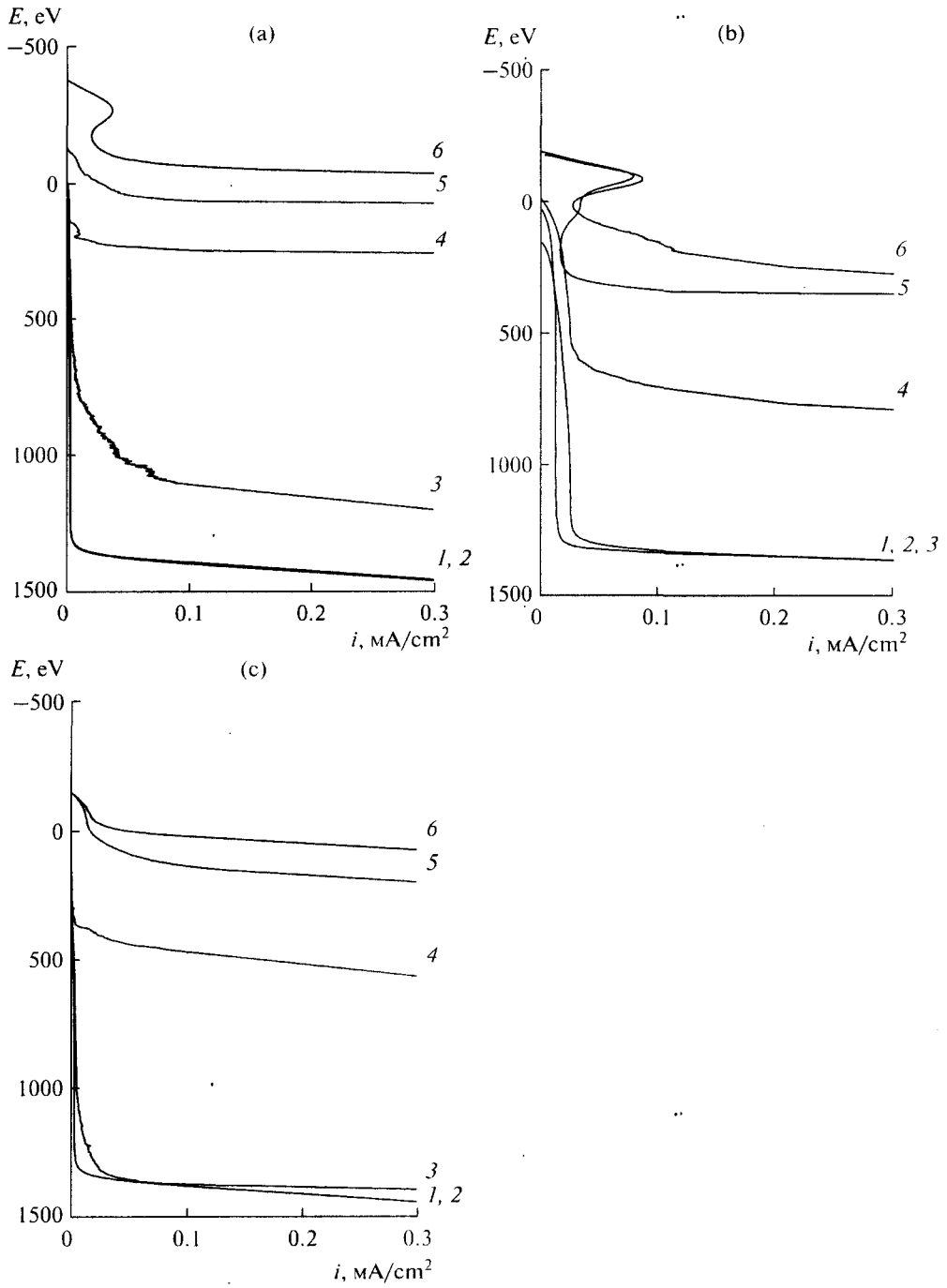

Fig. 6. Anodic curves on (a) Armco Fe, (b) cementite, and (c) Fe70Ti15C15 composite in borate solution with pH 7.4 containing NaCl additive, M: (*1*) 0, (*2*) 10^{-4}, (*3*) 10^{-3}, (*4*) 10^{-2}, (*5*) 0.1, and (*6*) 0.5.

Thus, the resistance of α-Fe + Fe_3C + TiC composites to local activation (in 10^{-2} M NaCl) increases with an increase in the cementite content; however, at a cementite concentration of more than 50 wt %, the composites are susceptible to depassivation. The resistance of $xFeO \cdot yTiO_2$ films on α-Fe + Fe_3C + TiC composites against local activation is lower than that of Fe_3O_4/γ-Fe_2O_3 (γ-FeOOH) films on α-Fe + Fe_3C composites.

CONCLUSIONS

Corrosion–electrochemical properties of α-Fe + Fe_3C + TiC three-phase nanocrystalline composites in borate solutions with pH 6.3–9.0 with or without NaCl are studied. α-Fe + Fe_3C + TiC composites are characterized by heightened resistance at the active-oxidation potentials of cementite and ferrite due to the surface formation of $xFeO \cdot yTiO_2$ mixed oxides. With an increase in the cementite content in the composites, the amount of $xFeO \cdot yTiO_2$ mixed oxides in the passive layer decreases.

Passive films based on $xFeO \cdot yTiO_2$ are already formed at the first stage of the oxidation of α-Fe + Fe_3C + TiC composites with a low cementite content. Protective properties of $xFeO \cdot yTiO_2$ films and their resistance to local activation are worse compared to those of $Fe_3O_4/\gamma\text{-}Fe_2O_3$ (γ-FeOOH) passive films formed on iron and α-Fe + Fe_3C composites.

ACKNOWLEDGMENTS

The work was supported by the programs of the Division of Physical Sciences "Physics of Novel Materials and Structures" and "Scientific Principles of Designing 3D Corrosion-Resistant Iron-Based Nanocomposite Materials Containing Poorly Soluble Inclusion Phases." We are grateful to O.M. Kanunnikova, senior scientist of the Physical Technical Institute, Ural Division of the Russian Academy of Sciencs, for her help in conducting X-ray photoelectron studies.

REFERENCES

1. Syugaev, A.V., Lomaeva, S.F., and Reshetnikov, S.M., *Fizikokhim. Poverkhn. Zashch. Mater.*, 2010, vol. 46, no. 1, p. 74. [Prot. Met. Phys. Chem. Surf. (Engl. Transl.), 2010, vol. 46, no. 1, p. 82].
2. Syugaev, A.V., Lomaeva, S.F., Lyalina, N.V., and Reshetnikov, S.M., *Fizikokhim. Poverkhn. Zashch. Mater.*, 2011, vol. 47, no. 3 p. 267. [Prot. Met. Phys. Chem. Surf. (Engl. Transl.), 2011, vol. 47, no. 3, p. 320].
3. Lomaeva, S.F., Povstugar, I.V., Volkov, V.A., et al., *Khim. Interesah Ustoich. Razvit.*, 2009, no. 6, p. 629.
4. Lomaeva, S.F., Maratkanova, A.N., Volkov, V.A., et al., *Khim. Fiz. Mezoskop.*, 2010, no. 1, p. 120.
5. Lomaeva, S.F., Volkov, V.A., Maratkanova, A.N., et al., *Materialovedenie*, 2010, no. 6, p. 58.
6. Syugaev, A.V., Lomaeva, S.F., Maratkanova, A.N., et al., *Fizikokhim. Poverkhn. Zashch. Mater.*, 2009, vol. 45, no. 1, p. 84. [Prot. Met. Phys. Chem. Surf. (Engl. Transl.), 2009, vol. 45, no. 1, p. 81].
7. Povstugar, V.I., Shakov, A.A., Mikhailova, S.S., et al., *Zh. Anal. Khim.*, 1998, vol. 53, no. 8, p. 795.
8. Syugaev, A.V., Lomaeva, S.F., and Reshetnikov, S.M., *Zashch. Met.*, 2008, vol. 44, no. 1, p. 58.
9. Yomoto, H., Nagamine, Y., Nagahama, J., and Shimotomai, M., *Vacuum*, 2002, vol. 65, p. 527.
10. Nefedov, V.N., *Rentgenoelektronnaya spektroskopiya khimicheskikh soedinenii* (X-ray Photoelectron Spectroscopy of Chemical Compounds), Moscow: Khimiya, 1984.
11. McIntyre, N.S. and Zetaruk, D.G., *Anal. Chem.*, 1977, vol. 49, no. 11, p. 1521.
12. *Practical Surface Analysis by Auger and X-ray Photoelectron Spectroscopy*, Briggs, D. and Seah, M.P., Eds., Chichester: Wiley, 1983.
13. Sukhotin, A.M., *Fizicheskaya khimiya passiviruyushchikh plenok na zheleze* (The Physical Chemistry of Passivating Films on Iron), Leningrad: Khimiya, 1989.
14. Kotenev, V.A., Chukalovskaya, T.V., and Chebotareva, N.P., *Zashch. Met.*, 1997, vol. 33, no. 2, p. 144.
15. Tyurin, A.G., *Termodinamika khimicheskoi i elektrokhimicheskoi ustoichivosti splavov. II. Nizkotemperaturnoe okislenie* (Thermodynamics of Chemical and Electrochemical Stability of Alloys. II. Low-Temperature Oxidation), Chelyabinsk: ChelGU, 2004.
16. Syugaev, A.V., Lomaeva, S.F., Reshetnikov, S.M., et al., *Fizikokhim. Poverkhn. Zashch. Mater.*, 2008, vol. 44, no. 4, p. 395.